Robotica: (2021) volume 39, pp. 233–249. © The Author(s), 2020. Published by Cambridge University Press.
doi:10.1017/S026357472000034X

Dimensional Synthesis and Performance Evaluation of Four Translational Parallel Manipulators

I. Ben Hamida†‡, M. A. Laribi†*, A. Mlika‡, L. Romdhane‡¶ and S. Zeghloul†

†*Department of GMSC, Pprime Institute, CNRS, University of Poitiers, ENSMA, UPR 3346, France.*
E-mails: ines.ben.hamida@univ-poitiers.fr, said.zeghloul@univ-poitiers.fr
‡*Mechanical Laboratory of Sousse, National Engineering School of Sousse, University of Sousse, Tunisia.*
E-mails: abdelfattah.mlika@eniso.u-sousse.tn, lotfi.romdhane@gmail.com, lromdhane@aus.edu
¶*Department of Mechanical Engineering, American University of Sharjah, PO Box 26666 Sharjah, UAE*

(Accepted May 3, 2020. First published online: June 22, 2020)

SUMMARY
The optimum selection of a structure for a given application is a capital phase in typological synthesis of parallel robots. To help in this selection, this paper presents a performance evaluation of four translational parallel robots: Delta, 3-UPU, Romdhane-Affi-Fayet, and Tri-pyramid (TP). The problem is set as a multiobjective optimization using genetic algorithm methods, which uses kinematic criteria, that is, global dexterity and compactness, to ensure a prescribed workspace. The results are presented as Pareto fronts, which are used to compare the performances of the aforementioned structures. The obtained results show that the TP robot has the best kinematic performance, whereas the 3-UPU robot is the most compact for a given prescribed workspace.

KEYWORDS: Dimensional synthesis; Compactness; Dexterity; Genetic algorithm.

1. Introduction

In the last decades, there was an increasing interest in parallel robots due to their excellent accuracy relative to serial robots. However, the parallel architectures with six Degree Of Freedom (DOF) have complex kinematic and dynamic models, which led some researchers to present parallel structures with less than six DOFs. Moreover, several applications do not require six DOFs. Therefore, translational parallel manipulators (TPMs) became popular for their ease of modeling and for their wide range of applications (e.g., pick and place tasks, machining and assembly operations).[1–5] Among more than 100 TPMs in the literature, very few of them have been commercialized like the well-known Delta robot.[6]

The design problem of parallel robots has been the subject of extensive research activities in recent years. One of the dimensional design approaches is the one based on minimizing an objective function. It consists of establishing a cost function for the criterion to optimize and associate the appropriate constraints with the problem.

Interval analysis method has been widely used for solving optimization problems. Chablat et al.[7] used this method to compare two 3-DOF TPMs to obtain the largest dexterous workspace. Another

* Corresponding author. E-mail: med.amine.laribi@univ-poitiers.fr

method based on an exhaustive search algorithm was used by Stock et al.[8] to optimize the workspace and the manipulability of a linear Delta manipulator.

The work of Yunjiang Lou et al.[9] deals with different nonlinear optimization algorithms to find the optimal design of two parallel manipulators: the Delta robot and the Gough–Stewart platform. Five algorithms were investigated: the sequential quadratic programming, the controlled random search, the genetic algorithm (GA), the differential evolution, and the particle swarm optimization. The study showed that there is no a unique best method but a suitable algorithm can be selected as a function of the nature of the problem. Kelaiaia et al.[10] applied a methodology for dimensional synthesis to a linear Delta robot, based on multiobjective optimization of a geometric criterion versus kinematic and dynamic performances. Another work by the same authors[11] was interested in the analysis and comparison of two optimization approaches: the single-objective and the multiobjective optimization. This study showed that the multiobjective approach based on non dominated sorting genetic algorithm (non-dominated sorting-based GA) is more effective than the single-objective one, since it enables to find a compromise between several performances even when they are antagonist. Jamwal et al.[12] proposed an optimization of a soft parallel manipulator dedicated to rehabilitation, using a modified GA, where the objective was the minimization of the global conditioning number. Laribi et al.[13] presented the mathematical concept of power of a point as a criterion of the geometric optimization of the Delta robot for a prescribed workspace using GA. The same concept was used for a robust optimization of the Romdhane-Affi-Fayet (RAF) robot to have a specified workspace and a high dexterity.[14]

This paper presents a new approach to develop the mathematical model of the TPMs workspace without the need to solve the geometric model. The efficiency of this new workspace formulation is illustrated through four TPMs with different topologies: Delta, 3-UPU, RAF, and Tri-pyramid (TP). These translational structures present different shapes of legs' workspace and different types of actuation. The 3-UPU, the RAF, and the TP have linear actuation and the Delta has rotary actuation. Because of the diversity in the designs of the TPMs, it is difficult to find a common ground to compare all these structures, and this work handles candidates with topologies covering a large panel.

The objective consists of finding the optimal design of each of these robots, which allows them to access a prescribed workspace with the smallest size and the highest dexterity. A multiobjective genetic algorithm (MOGA) will be used for the optimization problem.

The architectural and design parameters of the four robots are presented in Section 2. The formulation of the dimensional optimization problem for the four robots is established in Section 3. The obtained results, discussion, and comparison are presented in Section 4. Finally, some conclusions and perspectives of this work are given in the last section.

2. Geometric and Kinematic Study of Translational Robots

In this section, we present the four studied robot structures: their geometric and kinematic models as well as their workspaces. The mathematical evaluation of the manipulators' workspaces will be determined through the power of a point concept used in refs. [13, 14]. This approach has been the subject of a previous work.[15]

2.1. The Delta robot

The Delta robot is the most known and commercialized TPM. Its originality resides in the use of three parallelogram structures to restrain the rotations of the mobile platform. As shown in Fig. 1(a), the Delta robot consists of three identical legs, each one is composed of two successive parallel revolute joints relating the base to the parallelogram structure. The mobile platform is connected by three revolute joints to the three parallelograms.

The structural design parameters are L_1, L_2, r_b, r_p, α_1, α_2, and α_3, where L_1 and L_2 are the arms' lengths, r_b and r_p are, respectively, the radius of the base and the mobile platform, and α_i are the intersection angles between $\mathbf{OA_i}$ and the axis $\mathbf{X}$ as shown in Fig. 1(b). φ_{1i} are the input rotations of the three legs, whereas φ_{2i} and φ_{3i} are the passive rotations ($i = 1, 2, 3$).

2.1.1. Geometric model and Jacobian matrix. The geometric model of the Delta robot can be obtained through the closed loop equation of one leg. Then, the position of the mobile platform is given by the following equation where X_P, Y_P, and Z_P are the coordinates of the point P in the reference frame $R(O, \mathbf{X}, \mathbf{Y}, \mathbf{Z})$ (see Fig. 1(b)).

https://doi.org/10.1017/S026357472000034X Published online by Cambridge University Press

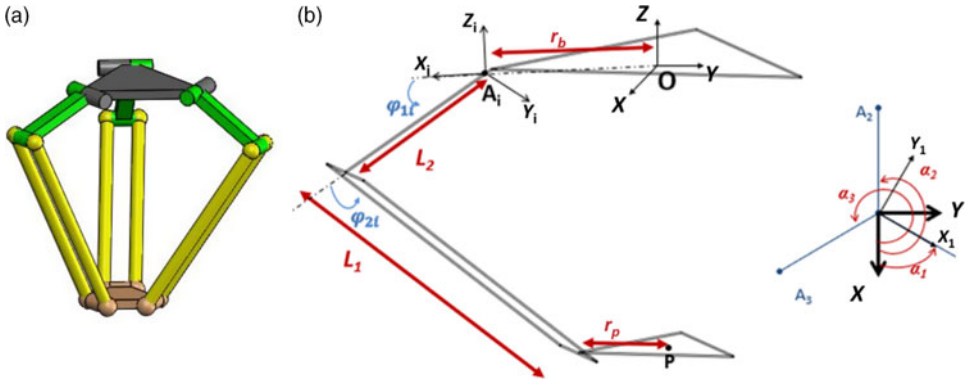

Fig. 1. The Delta robot: (a) CAD model and (b) parameters of one leg.

$$\begin{cases} X_P = \cos\alpha_i \left(r_b + L_2\cos\varphi_{1i} + L_1\cos\varphi_{3i}\cos\left(\varphi_{1i}+\varphi_{2i}\right) - r_p\right) - L_1\sin\alpha_i\sin\varphi_{3i} \\ Y_P = \sin\alpha_i \left(r_b + L_2\cos\varphi_{1i} + L_1\cos\varphi_{3i}\cos\left(\varphi_{1i}+\varphi_{2i}\right) - r_p\right) + L_1\cos\alpha_i\sin\varphi_{3i} \\ Z_P = L_2\sin\varphi_{1i} + L_1\cos\varphi_{3i}\sin\left(\varphi_{1i}+\varphi_{2i}\right) \end{cases}$$
$$i = 1, 2, 3 \tag{1}$$

By squaring and addition of these equations, the passive variables are eliminated and the direct geometric model is obtained in Eq. (2).

$$[B_i - X_P]^2 + [C_i - Y_P]^2 + [D_i - Z_P]^2 = {L_1}^2 \tag{2}$$

where $B_i = (r + L_2\cos\varphi_{1i})\cos\alpha_i$, $C_i = (r + L_2\cos\varphi_{1i})\sin\alpha_i$, $D_i = -L_2\sin\varphi_{1i}$

$$i = 1, 2, 3 \quad \& \quad r = r_b - r_p$$

The kinematic model of the Delta robot, Eq. (3), is obtained by differentiating Eq. (2) with respect to time.

$$\begin{aligned} &\dot{X}_P\left(X_P - B_i\right) + \dot{Y}_P\left(Y_P - C_i\right) + \dot{Z}_P\left(Z_P - D_i\right) \\ &= \dot{B}_i\left(X_P - B_i\right) + \dot{C}_i\left(Y_P - C_i\right) + \dot{D}_i\left(Z_P - D_i\right) \end{aligned} \tag{3}$$

where $\dot{B}_i = -L_2\cos\alpha_i\sin\varphi_{1i}\,\dot{\varphi}_{1i}$, $\dot{C}_i = -L_2\sin\alpha_i\sin\varphi_{1i}\,\dot{\varphi}_{1i}$, and $\dot{D}_i = -L_2\cos\varphi_{1i}\,\dot{\varphi}_{1i}$

By rearranging the three equations in a matrix form, we obtain the Jacobian matrix $\mathbf{J}$.

$$\mathbf{J} = \mathbf{J_P}\left(\mathbf{J_\varphi}\right)^{-1} \tag{4}$$

where

$$\mathbf{J_P} = \begin{pmatrix} X_P - B_1 & Y_P - C_1 & Z_P - D_1 \\ X_P - B_2 & Y_P - C_2 & Z_P - D_2 \\ X_P - B_3 & Y_P - C_3 & Z_P - D_3 \end{pmatrix}, \qquad \mathbf{J_\varphi} = \begin{pmatrix} J_{xx} & 0 & 0 \\ 0 & J_{yy} & 0 \\ 0 & 0 & J_{zz} \end{pmatrix}$$

$$J_{xx} = -L_2\left[\cos\alpha_1\left(X_P - B_1\right) + \sin\alpha_1\left(Y_P - C_1\right)\right]\sin\varphi_{11} - L_2\left(Z_P - D_1\right)\cos\varphi_{11}$$

$$J_{yy} = -L_2\left[\cos\alpha_2\left(X_P - B_2\right) + \sin\alpha_2\left(Y_P - C_2\right)\right]\sin\varphi_{12} - L_2\left(Z_P - D_2\right)\cos\varphi_{12}$$

$$J_{zz} = -L_2\left[\cos\alpha_3\left(X_P - B_3\right) + \sin\alpha_1\left(Y_P - C_3\right)\right]\sin\varphi_{13} - L_2\left(Z_P - D_3\right)\cos\varphi_{13}$$

2.1.2. Workspace evaluation. The workspace of the Delta robot is given by the intersection of three volumes generated by the three legs. The workspace generated by the *i*th leg is a torus of center A_i

https://doi.org/10.1017/S026357472000034X Published online by Cambridge University Press

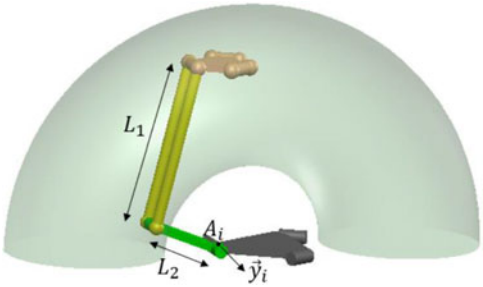

Fig. 2. The workspace of one leg of the Delta robot.

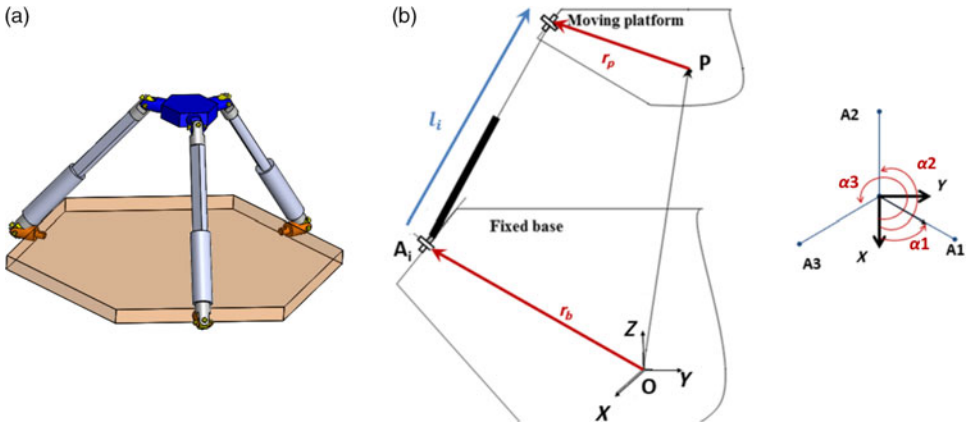

Fig. 3. The 3-UPU robot: (a) CAD model and (b) parameters of one leg.

and axis $\mathbf{Y_i}$ where $R_i(A_i, \mathbf{X_i}, \mathbf{Y_i}, \mathbf{Z_i})$ is a fixed frame corresponding to the *i*th leg (see Fig. 2). L_2 and L_1 are, respectively, the minor and major radii of the torus given in Eq. (5).

$$\left({x_{P_i}}^2 + {y_{P_i}}^2 + {z_{P_i}}^2 + {L_2}^2 - {L_1}^2\right)^2 = 4{L_2}^2\left({x_{P_i}}^2 + {z_{P_i}}^2\right) \tag{5}$$

where

$$x_{P_i} = \cos\alpha_i X_P + \sin\alpha_i Y_P - r,\ y_{P_i} = -\sin\alpha_i X_P + \cos\alpha_i Y_P,\ z_{P_i} = Z_P$$

Thus, the limits of the workspace can be given by the following function:

$$F_i{}^{DELTA}(P) = \left({x_{P_i}}^2 + {y_{P_i}}^2 + {z_{P_i}}^2 + {L_2}^2 - {L_1}^2\right)^2 - 4{L_2}^2\left({x_{P_i}}^2 + {z_{P_i}}^2\right)$$
$$i = 1, 2, 3 \tag{6}$$

2.2. The 3-UPU robot

The 3-UPU is TPM proposed by Tsai in 1996.[16] It consists of three identical legs with three linear actuators. Each leg is composed of a sequence of three joints U, P, and U (U: universal joint, P: prismatic joint) as shown in Fig. 3(a).

The design parameters and joint variables are given in Fig. 3(b) where r_b and r_p are, respectively, the radii of the base and the mobile platform and α_i are the intersection angles between $\mathbf{OA_i}$ and the axis $\mathbf{X}$. The actuators positions are parametrized by $\mathbf{l_i}$ ($i = 1, 2, 3$).

2.2.1. Geometric model and Jacobian matrix. The geometric model can be defined through the closed loop equation of one leg given by the vector $\mathbf{OP}$.

$$\mathbf{OP} = \mathbf{r_b} + \mathbf{l_i} - \mathbf{r_p}, \qquad i = (1, 2, 3) \tag{7}$$

https://doi.org/10.1017/S026357472000034X Published online by Cambridge University Press

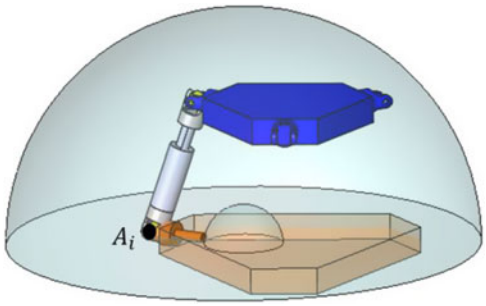

Fig. 4. The workspace of one leg of the 3-UPU robot.

By decomposing this equation on the reference frame $R(O, \boldsymbol{X}, \boldsymbol{Y}, \boldsymbol{Z})$, we obtain the coordinates of the mobile platform.

$$\begin{cases} X_P = r_b \cos\alpha_i + l_{ix} - r_p \cos\alpha_i \\ Y_P = r_b \sin\alpha_i + l_{iy} - r_p \sin\alpha_i \\ Z_P = l_{iz} \end{cases} \tag{8}$$

Then, the inverse geometric model is obtained by squaring and summing the previous equations.

$$l_i = \sqrt{(X_P - r\cos\alpha_i)^2 + (Y_P - r\sin\alpha_i)^2 + (Z_P)^2} \tag{9}$$

where $r = r_b - r_p$ and $i = 1, 2, 3$

The inverse kinematic model is obtained by differentiating Eq. (9) with respect to time.

$$\begin{pmatrix} \dot{l}_1 \\ \dot{l}_2 \\ \dot{l}_3 \end{pmatrix} = \begin{pmatrix} \frac{X_P - r\cos\alpha_1}{l_1} & \frac{Y_P - r\sin\alpha_1}{l_1} & \frac{Z_P}{l_1} \\ \frac{X_P - r\cos\alpha_2}{l_2} & \frac{Y_P - r\sin\alpha_2}{l_2} & \frac{Z_P}{l_2} \\ \frac{X_P - r\cos\alpha_3}{l_3} & \frac{Y_P - r\sin\alpha_3}{l_3} & \frac{Z_P}{l_3} \end{pmatrix} \begin{pmatrix} \dot{X}_P \\ \dot{Y}_P \\ \dot{Z}_P \end{pmatrix} \tag{10}$$

Thus, the Jacobian matrix is given by the following equation

$$\mathbf{J} = \begin{pmatrix} \frac{X_P - r\cos\alpha_1}{l_1} & \frac{Y_P - r\sin\alpha_1}{l_1} & \frac{Z_P}{l_1} \\ \frac{X_P - r\cos\alpha_2}{l_2} & \frac{Y_P - r\sin\alpha_2}{l_2} & \frac{Z_P}{l_2} \\ \frac{X_P - r\cos\alpha_3}{l_3} & \frac{Y_P - r\sin\alpha_3}{l_3} & \frac{Z_P}{l_3} \end{pmatrix} \tag{11}$$

2.2.2. Workspace evaluation. The workspace generated by one leg of the 3-UPU robot (see Fig. 4) is the volume limited by two concentric spheres of center A_i and radii $l_{\max}$ and $l_{\min}$ corresponding, respectively, to the upper and lower limits of the extension of the actuator. Thus, the workspace boundaries are defined through Eqs. (12) and (13).

$$F_{i\_\max}{}^{3UPU} = (X_P - r\cos\alpha_i)^2 + (Y_P - r\sin\alpha_i)^2 + {Z_P}^2 - l_{\max}^2 \tag{12}$$

$$F_{i\_\min}{}^{3UPU} = (X_P - r\cos\alpha_i)^2 + (Y_P - r\sin\alpha_i)^2 + {Z_P}^2 - l_{\min}^2 \tag{13}$$

$$i = (1, 2, 3)$$

https://doi.org/10.1017/S026357472000034X Published online by Cambridge University Press

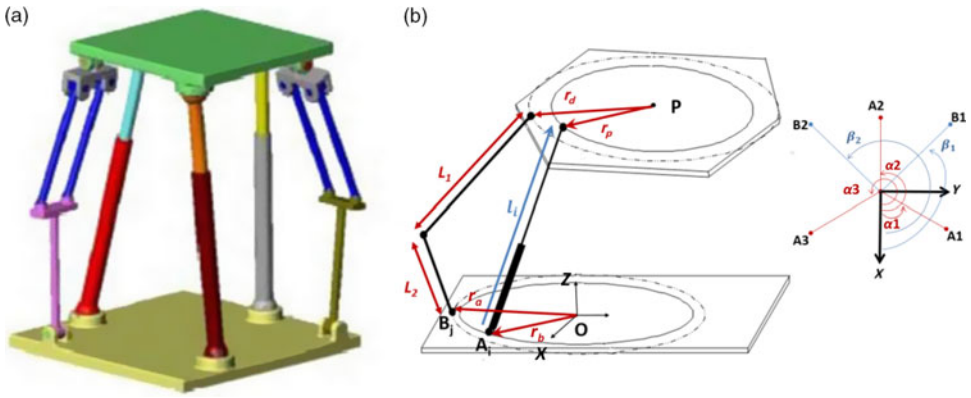

Fig. 5. The RAF robot: (a) CAD model and (b) parameters of one leg.

2.3. The RAF robot

The RAF robot is a TPM proposed by Romdhane et al.[4] It consists of a mobile platform related to a fixed base by three active legs and two passive kinematic chains used to prevent platform's rotations. The actuators are linear and are connected to the base and the mobile platform by two spherical joints (see Fig. 5(a)).

Figure 5(b) presents the design parameters and joint variables of the RAF robot. For the active legs, we consider r_b and r_p are the radii of the base and the mobile platform, respectively, and $l_i\,(i = 1, 2, 3)$ are the input motion. L_1 and L_2 are the lengths of the arms of the passive chains and r_a and r_d are the radii of the base and the mobile platform, respectively.

2.3.1. Geometric model and Jacobian matrix. Due to the similarity between the active part of the RAF robot and the 3-UPU robot, the geometric model is determined by the same way.

$$l_i = \sqrt{(X_P - r\cos\alpha_i)^2 + (Y_P - r\sin\alpha_i)^2 + (Z_P)^2} \tag{14}$$

where $r = r_b - r_p$ and $i = (1, 2, 3)$

X_P, Y_P, and Z_P are the coordinates of the center of the mobile platform in the reference frame R (O, X, Y, Z).

The Jacobian matrix of the RAF robot given in Eq. (15) is obtained by differentiating the inverse geometric model with respect to time.

$$\mathbf{J} = \begin{pmatrix} \dfrac{X_P - r\cos\alpha_1}{l_1} & \dfrac{Y_P - r\sin\alpha_1}{l_1} & \dfrac{Z_P}{l_1} \\ \dfrac{X_P - r\cos\alpha_2}{l_2} & \dfrac{Y_P - r\sin\alpha_2}{l_2} & \dfrac{Z_P}{l_2} \\ \dfrac{X_P - r\cos\alpha_3}{l_3} & \dfrac{Y_P - r\sin\alpha_3}{l_3} & \dfrac{Z_P}{l_3} \end{pmatrix} \tag{15}$$

2.3.2. Workspace evaluation. The workspace of the RAF robot is made by the intersection of two regions: active and passive workspaces presented in Fig. 6.

The resemblance between the active legs and the 3-UPU legs leads to the same equations for the active workspace limits.

$$F_{i_{\max}}{}^{RAF}(P) = (X_P - r\cos\alpha_i)^2 + (Y_P - r\sin\alpha_i)^2 + {Z_P}^2 - l_{\max}^2 \tag{16}$$

$$F_{i_{\min}}{}^{RAF}(P) = (X_P - r\cos\alpha_i)^2 + (Y_P - r\sin\alpha_i)^2 + {Z_P}^2 - l_{\min}^2 \tag{17}$$

$$i = (1, 2, 3)$$

https://doi.org/10.1017/S026357472000034X Published online by Cambridge University Press

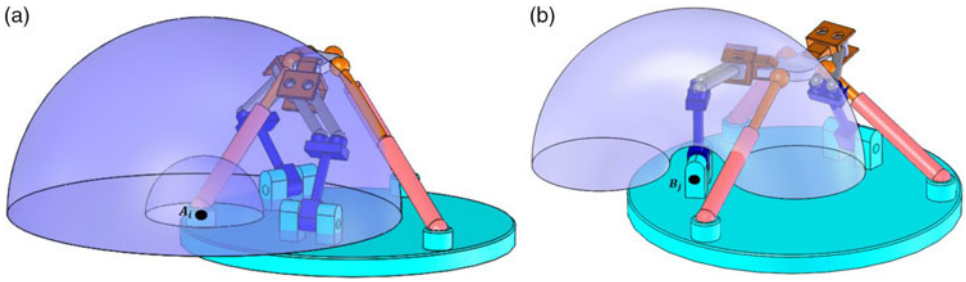

Fig. 6. The workspace of one leg of the RAF robot: (a) active leg and (b) passive leg.

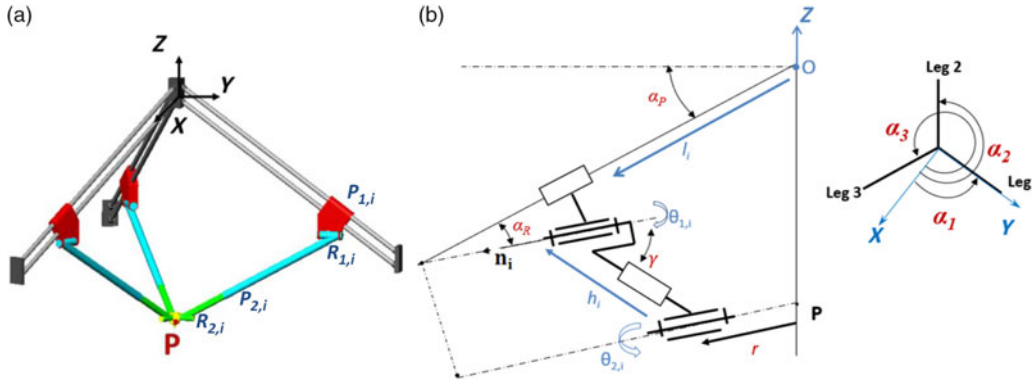

Fig. 7. The TP robot: (a) CAO and (b) parameters of one leg.

Equivalently, the similarity of passive chains and the Delta robot legs leads to the following equation for passive workspace.

$$F_j{}^{RAF}(P) = \left(x_{P_j}{}^2 + y_{P_j}{}^2 + z_{P_j}{}^2 + L_2{}^2 - L_1{}^2\right)^2 - 4L_2{}^2\left(x_{P_j}{}^2 + z_{P_j}{}^2\right)$$
$$j = 1, 2 \tag{18}$$

where $x_{P_j} = \cos\beta_j X_P + \sin\beta_j Y_P - e$, $y_{P_j} = -\sin\beta_j X_P + \cos\beta_j Y_P$, $z_{P_j} = Z_P$

$$e = r_a - r_d$$

2.4. The TP robot

The TP robot proposed by Zeng[17] consists of a mobile platform connected to a fixed base by three identical legs. For each leg, a prismatic joint is connecting two revolute joints and the whole is attached to the base by another prismatic joint (see Fig. 7).

The actuators are chosen to be fixed on the base on the first prismatic joint in order to ensure a high stiffness for the structure. This configuration gives the platform three degrees of freedom. To obtain a translational manipulator, the axes of the two rotational joints, in each leg, must be parallel.

2.4.1. Geometric model and Jacobian matrix. As shown in Fig. 7(b), the position of the mobile platform is given by $= \mathbf{r_0}$. The closed loop equation of each subchain is described by the following relation:

$$\boldsymbol{h_i} = \boldsymbol{l_i} - \boldsymbol{r_i} - \boldsymbol{r_0} \tag{19}$$

where:

$$\mathbf{r_0} = [X_P \; Y_P \; Z_P]^T$$

$$\mathbf{l_i} = l_i \left[\cos\alpha_p \cos\alpha_i \;\; \cos\alpha_p \sin\alpha_i \;\; \sin\alpha_p \right]^T$$

$$\mathbf{r_i} = r\left[\cos(\alpha_p - \alpha_R)\cos\alpha_i \;\; \cos(\alpha_p - \alpha_R)\sin\alpha_i \;\; \sin(\alpha_p - \alpha_R) \right]^T$$

https://doi.org/10.1017/S026357472000034X Published online by Cambridge University Press

By rewriting Eq. (19), we obtain the expression of $\mathbf{h_i}$.

$$\boldsymbol{h_i} = \begin{bmatrix} l_i \cos\alpha_p \cos\alpha_i - r \cos(\alpha_p - \alpha_R)\cos\alpha_i - X_P \\ l_i \cos\alpha_p \sin\alpha_i - r\cos(\alpha_p - \alpha_R)\sin\alpha_i - Y_P \\ l_i \sin\alpha_p - r\sin(\alpha_p - \alpha_R) - Z_P \end{bmatrix} \tag{20}$$

The kinematic position solutions are given by solving the following equation:

$$\boldsymbol{h_i}.\boldsymbol{r_i} = h_i.r.\cos(\gamma) \tag{21}$$

Eq. (21) is solved to give the actuators coordinates involving the platform coordinates.

$$l_i = \frac{A_i \cos^2\gamma - B_i \cos\alpha_R - r\cos\alpha_R \sin^2\gamma + \sqrt{\left[A_i \cos^2\gamma - B_i\cos\alpha_R - r\cos\alpha_R \sin^2\gamma\right]^2 - (\cos^2\gamma - \cos^2\alpha_R)\left(\cos^2\gamma\left({X_P}^2 + {Y_P}^2 + {Z_P}^2 + r^2 + 2rB_i\right) - (B_i + r)^2\right)}}{(\cos^2\gamma - \cos^2\alpha_R)} \tag{22}$$

where

$$A_i = (X_P \cos\alpha_i + Y_P \sin\alpha_i)\cos\alpha_P + Z_P \sin\alpha_P$$

$$B_i = (X_P \cos\alpha_i + Y_P \sin\alpha_i)\cos(\alpha_P - \alpha_R) + Z_P \sin(\alpha_P - \alpha_R)$$

The Jacobian matrix is obtained from the velocity equation, which is obtained from differentiating the kinematic position solution with respect to time.

$$\dot{l}_i = \frac{\boldsymbol{k_i}}{\frac{\boldsymbol{k_i}.\boldsymbol{l_i}}{l_i}} \begin{bmatrix} \dot{X}_P \\ \dot{Y}_P \\ \dot{Z}_P \end{bmatrix} \tag{23}$$

where $\boldsymbol{k_i} = \left(\frac{\boldsymbol{r_i}}{r} \times \frac{\boldsymbol{h_i}}{h_i}\right) \times \frac{\boldsymbol{h_i}}{h_i}$

The Jacobian matrix of the TP robot is given by Eq. (24).

$$\boldsymbol{J} = \begin{bmatrix} \boldsymbol{J_1} \\ \boldsymbol{J_2} \\ \boldsymbol{J_3} \end{bmatrix} \tag{24}$$

where $\boldsymbol{J_i} = \frac{\boldsymbol{k_i}}{\frac{\boldsymbol{k_i}.\boldsymbol{l_i}}{l_i}}$

2.4.2. Workspace evaluation. The workspace of the TP is obtained by the intersection of three volumes generated by the three legs. For each leg, the workspace is constrained by limits of the two prismatic joints l_i and h_i as shown in Fig. 8.

The volume generated by the first prismatic joint is a succession of conical surfaces given by the following equation. The reachable workspace of one leg is limited by two surfaces corresponding to $l_i = l_{\max}$ and $l_i = l_{\min}$.

$$F_{l_i}(P, l_i) = x_i^2 + y_i^2 - (z_i - r)^2(\tan\gamma)^2 \qquad i = 1, 2, 3 \tag{25}$$

where

$$\begin{cases} x_i = X_P \sin(\alpha_i) - Y_P \cos(\alpha_i) \\ y_i = -l_i \sin(\alpha_R) + Z_P \cos(\alpha_P - \alpha_R) - \sin(\alpha_P - \alpha_R)(X_P \cos(\alpha_i) + Y_P \sin(\alpha_i)) \\ z_i = l_i \cos(\alpha_R) - Z_P \sin(\alpha_P - \alpha_R) - \cos(\alpha_P - \alpha_R)(X_P \cos(\alpha_i) + Y_P \sin(\alpha_i)) \end{cases}$$

https://doi.org/10.1017/S026357472000034X Published online by Cambridge University Press

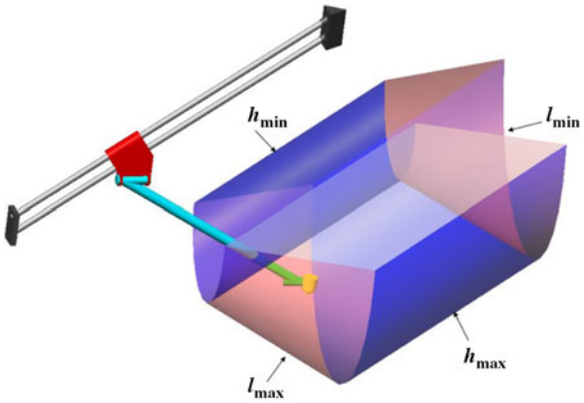

Fig. 8. The workspace of one leg of the TP robot.

In the following, we will consider the moving platform flat. Therefore, the angles α_P and α_R are equal. The equations of the bounding surfaces are given in Eqs. (26) and (27).

$$\begin{aligned} Fl_{i_{\min}}{}^{TP}(P) &= (X_P \ \sin\alpha_i - Y_P \ \cos\alpha_i)^2 + (Z_P - l_{\min}\sin\alpha_P)^2 \\ &\quad - (l_{\min}\cos\alpha_P - X_P \ \cos\alpha_i - Y_P \ \sin\ \alpha_i - r)^2(\tan\gamma)^2 \end{aligned} \tag{26}$$

$$\begin{aligned} Fl_{i_{\max}}{}^{TP}(P) &= (X_P \ \sin\alpha_i - Y_P \ \cos\alpha_i)^2 + (Z_P - l_{\max}\sin\alpha_P)^2 \\ &\quad - (l_{\max}\cos\alpha_P - X_P \ \cos\alpha_i - Y_P \ \sin\ \alpha_i - r)^2(\tan\gamma)^2 \end{aligned} \tag{27}$$

The motion of the passive prismatic joint generates a cylindrical volume bounded by the limits of the limb extension ($h_{\min}$ and $h_{\max}$). The corresponding equations of the two bounding surfaces are given by the following equation:

$$\begin{aligned} Fh_{i_{\min}}{}^{TP}(P) &= X_P^2 + Y_P^2 + Z_P^2 \\ &\quad - \frac{\left(\cos\alpha_p\cos\alpha_i X_P + \cos\alpha_p\sin\alpha_i Y_P + \sin\alpha_p \ Z_P\right)^2}{\left(\cos\alpha_p\cos\alpha_i\right)^2 + \left(\cos\alpha_p\sin\alpha_i\right)^2 + \left(\sin\alpha_p\right)^2} \\ &\quad - (h_{\min}\sin\gamma)^2 \end{aligned} \tag{28}$$

$$\begin{aligned} Fh_{i_{\max}}{}^{TP}(P) &= X_P^2 + Y_P^2 + Z_P^2 \\ &\quad - \frac{\left(\cos\alpha_p\cos\alpha_i \ X_P + \cos\alpha_p\sin\alpha_i \ \ Y_P + \sin\alpha_p \ Z_P\right)^2}{\left(\cos\alpha_p\cos\alpha_i\right)^2 + \left(\cos\alpha_p\sin\alpha_i\right)^2 + \left(\sin\alpha_p\right)^2} \\ &\quad - (h_{\max}\sin\gamma)^2 \end{aligned} \tag{29}$$

3. Dimensional Synthesis of Translational Parallel Robots

3.1. Problem formulation

The aim of this section is to formulate an optimization problem suitable for all considered TPMs. The objective is to find a set of design parameters that guarantee the smallest size of the structure as well as the maximum dexterity distribution within a prescribed workspace. The optimization problem is stated as follows:

$$\begin{cases} \text{Maximize } F(I) = [F1(I)F2(I)]^T \\ \quad \text{Subject to } \ C_i(I, P) \le 0 \\ \quad\quad \mathbf{I} = [x_1, .., x_n] \\ \quad\quad x_{j\,\min} < x_j < x_{j\,\max} \end{cases}$$

https://doi.org/10.1017/S026357472000034X Published online by Cambridge University Press

Table I. Bounding intervals of the Delta design parameters.

	r_b	r_p	L_1	L_2	H
Min	5	5	5	5	10
Max	70	60	50	50	100

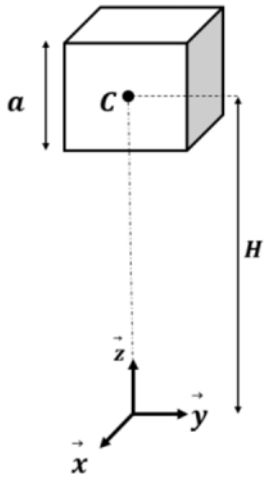

Fig. 9. The desired workspace.

where

P is a point belonging to the desired workspace.
$F(I)$ is vector containing the two objective functions defining the criteria to optimize
$C_i(I, P)$ are constraint functions
$x_1, .., x_n$ are the design variables of the robot, and $x_{j\,\min}$ and $x_{j\,\max}$ define the search domain for each variable x_j.

The considered desired workspace presented in Fig. 9 is defined by a set of vertices and can be considered in our case as a cube of length $\ll$ a $\gg$ and center $C(0, 0, H)$.

3.2. Design parameters

For each robot, a set of geometric parameters defining the structure was defined. The design vector will contain the geometric parameters of the robot and H, which defines the height of the cube with respect to the base (see Fig. 9).

- The Delta robot

  The design parameters of the Delta robot that are considered in the optimization problem are

  – r_b: is the base's radius
  – r_p: is the platform's radius
  – L_1: is the length of the parallelogram's arm
  – L_2: is the length of the arm linked to the base
  – H: is the position of the cube's center on Z-axis

The design vector is then given by $\mathbf{I} = \left[r_b, r_p\ , L_1, L_2, H\ \right]^T$. The bounding search interval for each parameter is given in Table I.

https://doi.org/10.1017/S026357472000034X Published online by Cambridge University Press

Table II. Bounding intervals of the 3-UPU design parameters.

	r_b	r_p	l_{max}	H
Min	5	5	0	1
Max	70	60	200	100

Table III. Bounding intervals of the RAF design parameters.

	r_b	r_p	l_{max}	r_a	r_d	L_1	L_2	H
Min	5	5	0	5	5	5	5	1
Max	70	60	200	60	60	50	50	100

- The 3-UPU robot

  For 3-UPU robot, four design parameters are considered:

  - r_b: is the base's radius
  - r_p: is the platform's radius
  - $l_{\max}$: is the maximum length of the prismatic joint
  - H : is the position of the cube's center on Z-axis

The design vector $\mathbf{I}$ is then given by $\mathbf{I} = \left[r_b, r_p, l_{\max}, H\right]^T$. The bounding search interval for each parameter is given in Table II.

- The RAF robot

The design vector of the RAF robot is composed of design parameters of the active legs and the design parameters of the passive kinematic chains defined below:

- r_b: is the base's radius of the active legs
- r_p: is the platform's radius of the active legs
- $l_{\max}$: is the maximum length of the active prismatic joint
- r_a: is the base's radius of the passive chains
- r_d: is the platform's radius of the passive chains
- L_1: is the length of the parallelogram's arm in the passive chains.
- L_2: is the length of the arm linked to the base in the passive chains.
- H: is the position of the cube's center on Z-axis.

The design vector is given by $I = \left[r_b,\ r_p,\ l_{\max}, r_a,\ r_d, L_1, L_2, H\right]^T$. The bounding search interval for each parameter is given in Table III.

- The TP robot

  The design parameters of the TP robot that are considered are

  - r: is the platform's radius
  - α_p: is the angle between the horizontal plane and the direction and the active prismatic joint
  - γ: is the angle between the axis of the first rotational joint and the direction and the passive prismatic joint
  - $l_{\max}$: is the maximum length of the active prismatic joint
  - $h_{\max}$: is the maximum length of the passive prismatic joint
  - H: is the position of the cube's center on Z-axis

The design vector is given by $I = \left[r, \alpha_p, \gamma, l_{\max}, h_{\max}, H\right]^T$. The bounding search interval for each parameter is given in Table IV.

https://doi.org/10.1017/S026357472000034X Published online by Cambridge University Press

Table IV. Bounding intervals of the Tri-pyramid design parameters.

	r	α_p	γ	l_{max}	h_{max}	H
Min	5	−70	−90	30	10	10
Max	70	0	0	200	100	100

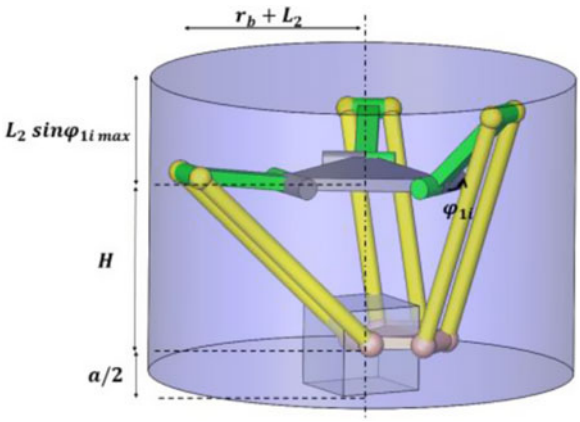

Fig. 10. The cylinder containing the Delta robot.

3.3. The objective functions

3.3.1. Compactness. Compactness function is evaluated by computing the ratio between the volume occupied by the structure and the volume of the desired workspace and expressed as follows:

$$C^{\%} = \frac{\text{desired workspace}}{\text{bounding cynlinder volume}} 100 \tag{30}$$

The bounding cylinder is the smallest cylinder containing the structure and every point within the desired workspace.

- The Delta robot

The cylinder containing the Delta robot is shown in Fig. 10. The corresponding function to compute the compactness criterion is given in Eq. (31)

$$C^{\%}{}_{\text{Delta}} = \begin{cases} \dfrac{a^3}{\pi.(r_b + L_2)^2 (H + \frac{a}{2})} & \text{if } \max\left(\varphi_{1i}(P_j)\right) \le 0 \\ \dfrac{a^3}{\pi.(r_b + L_2)^2 \left(H + \frac{a}{2} + L_2 \sin\left(\max\left(\varphi_{1i}(P_j)\right)\right)\right)} & \text{if } \max\left(\varphi_{1i}(P_j)\right) > 0 \end{cases} \tag{31}$$

where $i = 1, 2, 3$ and $j = 1,..,8$

- The 3-UPU robot

The compactness of the 3-UPU robot is given by the volume of the cylinder containing the structure (see Fig. 11). The objective function of compactness criterion is given by Eq. (32).

$$C^{\%}{}_{3-UPU} = \frac{a^3}{\pi.\, r_b{}^2 \left(H + \frac{a}{2}\right)} \tag{32}$$

- The RAF robot

The cylinder containing the RAF robot is presented in Fig. 12 and the corresponding compactness function is given by Eq. (33).

https://doi.org/10.1017/S026357472000034X Published online by Cambridge University Press

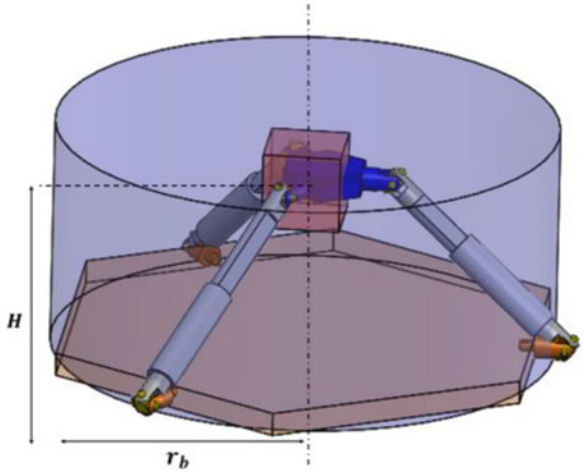

Fig. 11. The cylinder containing the 3-UPU robot.

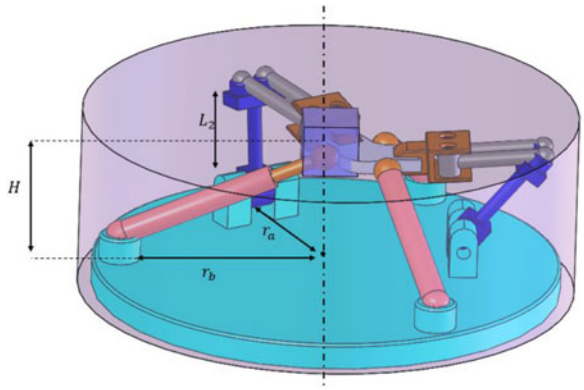

Fig. 12. The cylinder containing the RAF robot.

$$C^{\%}{}_{RAF} = \frac{a^3}{\pi\left(\max((r_a + L_2), r_b)\right)^2 \left(H + \frac{a}{2}\right)} \tag{33}$$

- The TP robot

The TP robot structure contained in the cylinder is shown in Fig. 13. The compactness function of the robot is given by Eq. (34).

$$C^{\%}{}_{TP} = \frac{a^3}{\pi\left(l_{\max} \cos \alpha_P\right)^2 \left(H + \frac{a}{2}\right)} \tag{34}$$

3.3.2. Dexterity. To describe the overall kinematic behavior of the robots, we use the error amplification factor, which is calculated using the inverse of the condition number $K(J)$, introduced by Gosselin.[18] The use of the condition number is not appropriate for manipulators having translational and rotational DOF. This problem of non-homogeneity of the Jacobean matrix is not encountered in our case, since this work deals only with translational robots.

$$\mu = \frac{1}{K(J)} \tag{35}$$

where, $K(J) = \|J\| \,.\, \left\|J^T\right\|$

https://doi.org/10.1017/S026357472000034X Published online by Cambridge University Press

Table V. Constraints functions of the four robots.

The Delta robot	$F_i{}^{DELTA}(P_j) \leq 0$	Torus equation
The 3-UPU robot	$F_{i_{\max}}{}^{3UPU}(P_j) \leq 0$	Exterior limit sphere
	$F_{i_{\min}}{}^{3UPU}(P_j) \geq 0$	Interior limit sphere
The RAF robot	$F_{i_{\max}}{}^{RAF}(P_j) \leq 0$	Exterior limit of the active workspace
	$F_{i_{\min}}{}^{RAF}(P_j) \geq 0$	Interior limit of the active workspace
	$F_k{}^{RAF}(P_j) \leq 0 \quad k = 1, 2$	Passive workspace
The TP robot	$Fl_{i_{\max}}{}^{TP}(P_j) \leq 0$	Limit surfaces of the active prismatic joint
	$Fl_{i_{\min}}{}^{TP}(P_j) \geq 0$	
	$Fh_{i_{\max}}{}^{TP}(P_j) \leq 0$	Limit surfaces of the passive prismatic joint
	$Fh_{i_{\min}}{}^{TP}\left(P_j\right) \geq 0$	

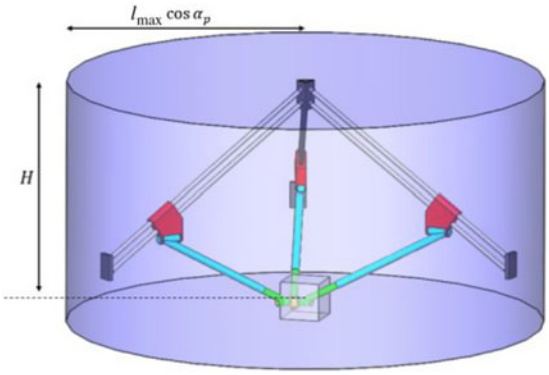

Fig. 13. The cylinder containing the TP robot.

To evaluate the global dexterity within the desired workspace, a global conditioning index ranging between 0 and 1 was defined in Eq. (36)

$$\mu_G = \frac{\sum_{j=1}^{N} \mu_j}{N} \tag{36}$$

where N is the discretization parameter of the desired workspace.

The best kinematic performance is reached when $\mu_G = 1$

The Jacobian matrices of the four robots have been defined in the previous section.

3.4. Constraint functions

Constraint functions are the functions defining the boundaries of the robot workspace. They depend on the joint's limits and types of each robot. Table V summarizes the constraint functions of the robots: $P_j (j = 1..8)$ are the desired cube vertices and $i = 1..3$ are the three legs of the robots. The point P_j belongs to the robot's workspace if it satisfies the following equations.

4. Results and Comparison

The problem was solved using the MOGA toolbox under Matlab software with the following parameters:

Population size	2000
Crossing probability	0.9
Probability of mutation	0.1

https://doi.org/10.1017/S026357472000034X Published online by Cambridge University Press

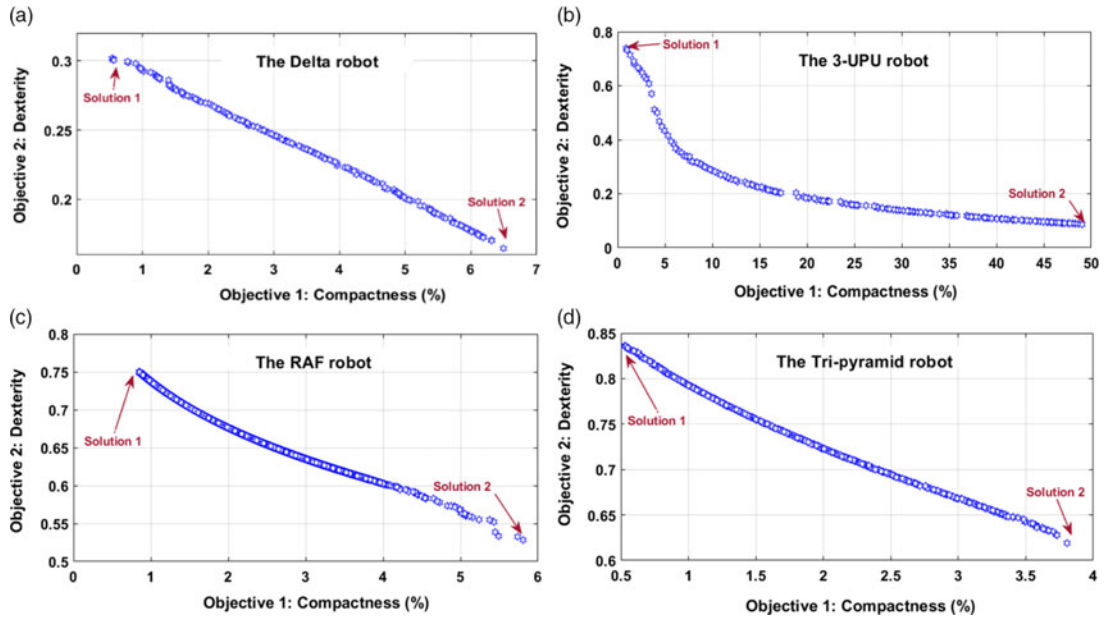

Fig. 14. Pareto front of the TPMs: (a) the Delta robot, (b) the 3-UPU robot, (c) the RAF robot, and (d) the TP robot.

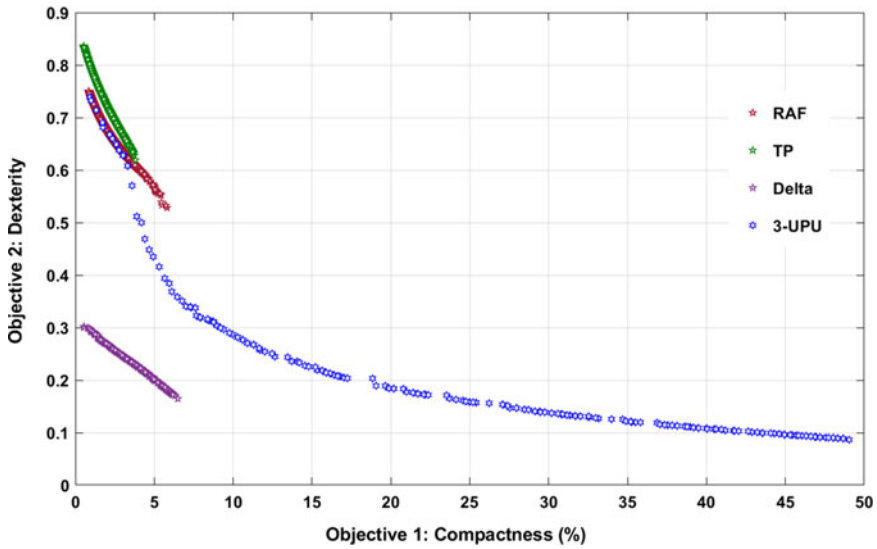

Fig. 15. Overlay of the four resulted Pareto fronts.

The cube's length was fixed at $a = 20$ mm. The obtained result for each robot is a Pareto front, which is a set of non-dominated optimal solutions that presents the best compromise between the two objectives. The Pareto front of the four robots is presented in Fig. 14.

It is noticed that there is a contradiction between the two objectives for the four robots; the improvement of the compactness yields the degradation of the dexterity and vice versa.

For the Delta robot, the compactness ranges between 0.5% and 7% whereas the dexterity ranges between 0.16 and 0.3, which is relatively low compared to RAF, UPU, and TP robots where the dexterity exceeds 0.7.

The 3-UPU robot has the largest range of variation for both dexterity (from 0.1 to 0.8) and compactness (from 0 to 50%); however, the solutions having a good dexterity higher than 0.5 correspond to a low compactness varying from 0 to 5% (see Fig. 15).

https://doi.org/10.1017/S026357472000034X Published online by Cambridge University Press

Table VI. Objective functions of the selected solutions.

	Delta		3-UPU		RAF		TP	
	Solution 1	**Solution 2**	**Solution 1**	**Solution 2**	**Solution 1**	**Solution 2**	**Solution 1**	**Solution 2**
$C^{\%}$	0.54	6.5	0.91	49.04	0.85	5.8	0.53	3.8
μ_G	0.3	0.16	0.74	0.08	0.75	0.53	0.84	0.62

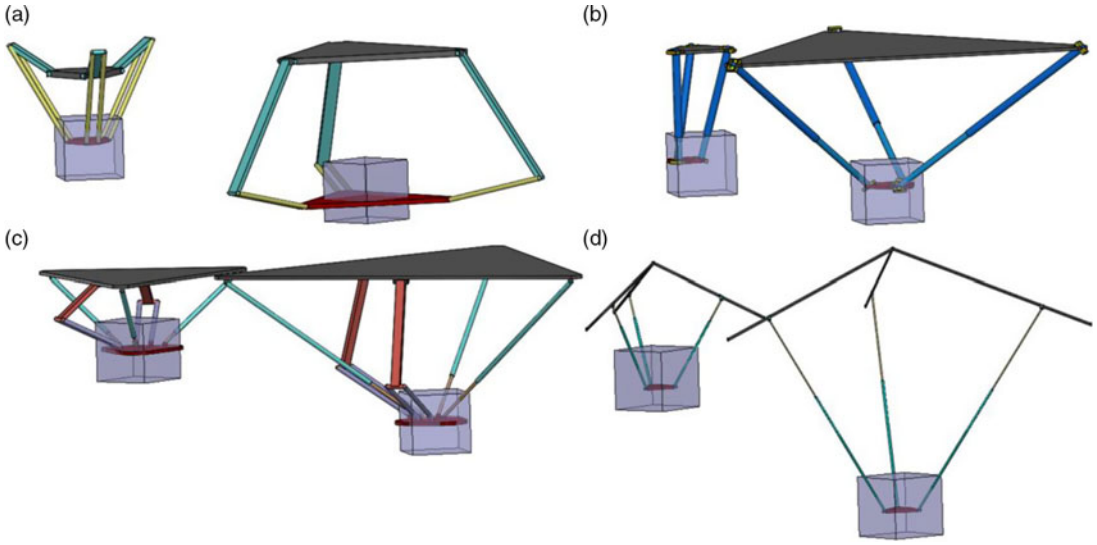

Fig. 16. CAD models of extreme solutions from the Pareto fronts: (a) the Delta robot, (b) the 3-UPU robot, (c) the RAF robot, and (d) the TP robot.

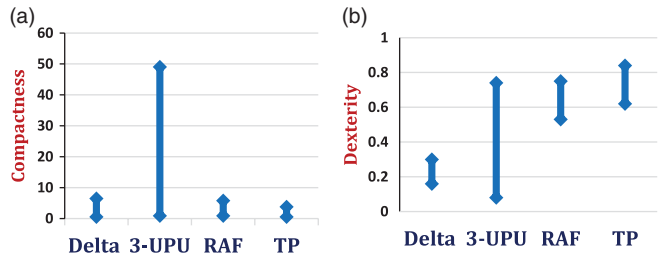

Fig. 17. Performances comparison of three translational parallel manipulators: (a) compactness and (b) dexterity.

For a better analysis, two solutions are selected from the Pareto front of each robot: the first one favoring the dexterity criterion (Solution 1) and the second favoring the compactness criterion (Solution 2). Their corresponding objective functions values are given in Table VI. The CAD's models of both solutions are presented in Fig. 16.

Figure 17 represents a comparative overview of the performances for the four robots. As it can be seen, the 3-UPU robot reached largely the best compactness with the value 49%; however, the three other robots have almost the same range that does not exceed 7%.

On the other hand, the TP robot has the best dexterity ranging between 0.62 and 0.84. The 3-UPU and RAF robots have practically the same maximum of dexterity equal to 0.75; however, the Delta robot has the poorest dexterity ranging between 0.16 and 0.3. The poor dexterity of the Delta robot can be explained by the use of rotary actuators.

5. Conclusion

In this work, we presented a multiobjective optimization approach of geometric and kinematic performances of four TPMs: Delta, 3UPU, RAF, and TP. The mathematical formulation of the problem

https://doi.org/10.1017/S026357472000034X Published online by Cambridge University Press

was defined by the maximization of two objective functions, that is, compactness and dexterity, for a desired workspace. The MOGA method was used to solve the problem. The obtained Pareto front for each robot shows that the two objective functions, that is, compactness and dexterity, are contradictory. The Pareto front presented the non-dominated solutions.

A comparison of the results of the four robot shows that there is no architecture that excels in both criteria. From a kinematic point of view, the TP robot has the highest dexterity with a global conditioning index ranging between 0.6 and 0.9. However, this architecture has the bulkiest structure with a compactness function that does not exceed 4%. The results show also that the 3-UPU robot has the best compactness, which can reach 50%. However, more than half of the corresponding Pareto front presents a poor dexterity, which does not exceed 0.2.

It is clear that no structure comes best in all cases of kinematic criteria and some recommendations to the designer on the choice of the structure, as a function of his application, represent one of the contributions of this work.

More criteria could be added, such as maximum required torque and stiffness, which will give more insight into the overall performance of these robots. In addition, combining typological and dimensional syntheses could be an interesting and challenging problem to be addressed as a future work.

Acknowledgment

This work is supported by the "Poitiers Université Foundation".

References

1. R. Clavel, "DELTA, A Fast Robot with Parallel Geometry," *Proceedings of 18th International Symposium on Industrial Robots 1988* (1988) pp. 91–100.
2. J. M. Hervé and F. Sparacino, "Star, a New Concept in Robotics," *International Conference 3K-ARK, Ferrara, Italy* (1992) pp. 176–183.
3. L. Tsai, G. C. Walsh and R. E. Stamper, "Kinematics of a Novel Three DOF Translational Platform," *Proceedings of the 1996 IEEE lntemational Conference on Robotics and Automation, Minneapolis, Minnesota* (1996) pp. 3446–3451.
4. L. Romdhane, Z. Affi and M. Fayet, "Design and singularity analysis of a 3-translational-DOF in-parallel manipulator," *J. Mech. Des.* **124**(3), 419–426 (2002).
5. X.-W. Kong and C. M. Gosselin, "Kinematics and singularity analysis of a novel type of 3-CRR 3-DOF translational parallel manipulator," *Int. J. Rob. Res.* **21**(9), 791–798 (2002).
6. I. Bonev, "Delta Parallel Robot—the Story of Success," The Parallel Mechanisms Information Center (2000) pp. 1–6.
7. D. C. Chablat, P. Wenger and J. Merlet, "A Comparative Study Between Two Three-DOF Parallel Kinematic Machines Using Kinetostatic Criteria and Interval Analysis," *Proceedings of the 11th World Congress in Mechanism and Machine Science* (2004) pp. 1–6.
8. M. Stock and K. Miller, "Optimal kinematic design of spatial parallel manipulators: Application to linear Delta robot," *J. Mech. Des.* **125**(2), 292 (2003).
9. L. Yunjiang, Z. Yongsheng, R. Huang, C. Xin and L. Zexiang, "Optimization algorithms for kinematically optimal design of parallel manipulators," *IEEE Trans. Autom. Sci. Eng.* **11**(2), 574–584 (2014).
10. R. Kelaiaia, O. Company and A. Zaatri, "Multiobjective optimization of a linear Delta parallel robot," *Mech. Mach. Theory* (50), 159–178 (2012).
11. R. Kelaiaia, A. Zaatri, O. Company and L. Chikh, "Some investigations into the optimal dimensional synthesis of parallel robots," *Int. J. Adv. Manuf. Technol.* **83**(9–12), 1525–1538 (2016).
12. P. K. Jamwal, S. Q. Xie, Y. H. Tsoi and K. C. Aw, "Forward kinematics modelling of a parallel ankle rehabilitation robot using modified fuzzy inference," *Mech. Mach. Theory* **45**(11), 1537–1554 (2010).
13. M. A. Laribi, L. Romdhane and S. Zeghloul, "Analysis and dimensional synthesis of the DELTA robot for a prescribed workspace," *Mech. Mach. Theory* **42**(7), 859–870 (2007).
14. M. A. Laribi, A. Mlika, L. Romdhane and S. Zeghloul, "Robust optimization of the RAF parallel robot for a prescribed workspace," *Mech. Mach. Sci.* (50), 383–393 (2018).
15. I. Ben Hamida, M. A. Laribi, A. Mlika, L. Romdhane and S. Zeghloul, "Geometric Based Approach for Workspace Analysis of Translational Parallel Robots," *ROMANSY 22 – Robot Design, Dynamics and Control. CISM International Centre for Mechanical Sciences*, vol. 584 (2019) pp. 180–188.
16. L.-W. Tsai, "Kinematics of a Three-DOF Platform with Three Extensible Limbs," **In:** *Recent Advances in Robot Kinematics* (J. Lenarèiè and V. Parenti-Castelli, eds.) (Kluwer Academic Publishers, 1996) pp. 401–410.
17. Q. Zeng, K. F. Ehmann and J. Cao, "Tri-pyramid robot: Design and kinematic analysis of a 3-DOF translational parallel manipulator," *Robot. Comput. Integr. Manuf.* **30**(6), 648–657 (2014).
18. C. Gosselin and J. Angeles, "A global performance index for the kinematic optimization of robotic manipulators," *J. Mech. Des.* **113**(3), 220 (1991).